Isothermal stress relaxation in electroplated Cu films. II. Kinetic modeling

Rui Huang[a)]
Department of Aerospace Engineering and Engineering Mechanics, University of Texas, Austin, Texas 78712

Dongwen Gan and Paul S. Ho
Laboratory for Interconnect and Packaging, University of Texas, Austin, Texas 78712

(Received 22 September 2004; accepted 21 March 2005; published online 13 May 2005)

In Part I we reported experimental results obtained from isothermal stress relaxation tests of electroplated Cu thin films with and without a passivation layer and deduced grain-boundary and interface diffusivities based on a kinetic model. Here in Part II we describe the detail of the model, which is based on coupling of grain-boundary diffusion with surface diffusion for unpassivated films and with interface diffusion for passivated films. Numerical solutions are obtained for the coupled diffusion problems and analytical solutions are obtained for several limiting cases. The effects of surface diffusivity and interface diffusivity on stress relaxation of polycrystalline thin films are analyzed and compared with experiments. The model predicts a transient behavior of stress relaxation and provides a quantitative correlation between stress relaxation and the kinetics of mass transport. In particular, the models can be used together with isothermal stress relaxation tests to characterize interface diffusion and to evaluate selected cap layers for improving electromigration reliability of Cu interconnects. © *2005 American Institute of Physics*. [DOI: 10.1063/1.1904721]

I. INTRODUCTION

In Part I of this study, a set of isothermal stress relaxation tests was conducted to measure grain-boundary and interface diffusivities in electroplated Cu films, which provides a useful method to evaluate the effectiveness of different cap layers and chemical-mechanical planarization (CMP) processes for improving electromigration (EM) reliability of Cu interconnects. A kinetic model is required for quantitative correlation between the measured stress relaxation data and the corresponding diffusivities. In general, stress in thin films can be relaxed by multiple mechanisms, such as dislocation plasticity[1] and diffusional creep[2] as well as voiding and cracking under tension[3] and delamination-buckling under compression.[4] Here we focus our attention on the diffusion mechanism, which is most relevant to EM reliability in Cu interconnects. Several authors have shown that, at moderate temperatures, stresses in polycrystalline thin films can be relaxed by diffusional flow of matter between the free surface and grain boundaries.[5–7] For a Cu film passivated with a cap layer, stress can be relaxed by mass transport between the interface and grain boundaries. Electromigration studies in Cu line structures showed that mass transport is dominated by diffusion at the interface between Cu and the cap layer, probably due to the presence of defects induced by CMP.[8,9] Recently, effects of cap layers on stress relaxation of Cu interconnect lines were observed experimentally[10,11] which indicates the coupling of interface diffusion and grain-boundary diffusion as a stress relaxation mechanism in passivated Cu films. Figure 1 schematically illustrates the structure and diffusion paths in unpassivated and passivated thin films, where the film ideally consists of one layer of grains with the grain boundaries perpendicular to the film-substrate interface.

The coupling between surface and grain-boundary diffusion has been studied previously. For example, Rice and Chuang[12] formulated a theory for diffusive cavity growth at grain boundaries. Genin *et al.*[13] analyzed the effect of stress on grain-boundary grooving by superimposing a solution corresponding to the steady-state grain-boundary diffusion to Mullin's solution of grain-boundary grooving. Antipov and Gao[14] developed a model for stress-induced atomic diffusion from a surface into a semi-infinite grain boundary. For unpassivated polycrystalline thin films, Thouless[15] developed a model coupling surface diffusion and a steady-state grain-boundary diffusion. Recently, Gao and co-workers[16,17] developed a model coupling surface diffusion and a constrained grain-boundary diffusion, also for unpassivated films, but accounting for the transient behavior of grain-boundary diffusion and the nonsliding condition at the film-substrate interface. For passivated films, however, we are not aware of any previous study on the coupling of grain-boundary diffusion and interface diffusion. Bower *et al.*[18] recently conducted numerical simulations of stress relaxation in a damascene Cu interconnect considering diffusion at grain boundaries and interfaces between Cu and surrounding layers.

This paper develops a kinetic model for stress relaxation in unpassivated and passivated polycrystalline thin films based on coupling of grain-boundary diffusion with surface and interface diffusion, respectively. For unpassivated films, the model differs from Thouless's model[15] in that the transient behavior of grain-boundary diffusion is explicitly considered, and differs from the model of Gao and co-workers[16,17] in that an approximation is made in calculating the normal stress at the grain boundary, which leads to a

[a)]Electronic mail: ruihuang@mail.utexas.edu

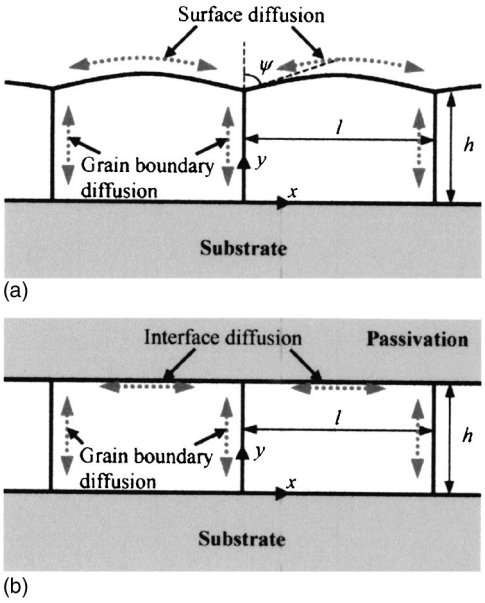

FIG. 1. Schematics of polycrystalline thin films: (a) an unpassivated film and (b) a passivated film.

simplified equation for grain-boundary diffusion and analytical solutions at limiting cases. For passivated films, the model couples the grain-boundary diffusion with interface diffusion and demonstrates the effect of a cap layer on stress relaxation. In Part I, the model has been used to analyze experimental results from isothermal stress relaxation tests of electroplated Cu thin films with and without a passivation layer, which allowed quantitative determination of the interface and grain-boundary diffusivities that control the electromigration reliability of Cu interconnects. This paper describes the detail of the kinetic model. Section II considers stress relaxation in an unpassivated film, and Sec. III considers a passivated film. The effects of surface and interface diffusivities on stress relaxation in unpassivated and passivated films are analyzed, respectively. Section IV discusses the limitations of the present model in comparison with experiments.

II. UNPASSIVATED FILMS: COUPLING OF GRAIN-BOUNDARY DIFFUSION AND SURFACE DIFFUSION

As shown in Fig. 1, we assume that a film consists of two-dimensional grains of a constant length l with grain boundaries of height h perpendicular to the film/substrate interface. For an unpassivated film [Fig. 1(a)], atoms diffuse along grain boundaries and the free surface. The atomic diffusion is driven by the gradient of chemical potential. The chemical potentials at the free surface and the grain boundary are, respectively,

$$\mu_S = \mu_0 - \kappa(s)\gamma_S\Omega, \tag{1}$$

$$\mu_B = \mu_0 - \sigma_B(y)\Omega, \tag{2}$$

where μ_0 is a reference value, γ_S is the surface energy density, Ω is the atomic volume, κ is the surface curvature, σ_B is the normal stress at the grain boundary, y is the coordinate along the grain boundary, and s is the curvilinear coordinate along the surface. The contribution of the elastic strain energy to the surface chemical potential has been neglected as Rice and Chuang[12] have shown that the contribution from the surface energy is much more significant in similar cases. In this study we ignore lattice diffusion and interface diffusion between the film and the substrate.

A. Equilibrium state

At equilibrium, the chemical potential is uniform. Consequently, the surface of each grain has a uniform curvature, i.e., $\kappa(s)=\kappa_0$, and the normal stress at each grain boundary is a constant, i.e., $\sigma_B(y)=\sigma_{B0}$. By a simple geometric consideration, the surface curvature at equilibrium is given by

$$\kappa_0 = -\frac{2\cos\psi}{l}, \tag{3}$$

where ψ is the dihedral angle at the intersection between a grain boundary and the surface, determined by the balance of local surface tension according to $2\gamma_S\cos\psi=\gamma_B$, where γ_B is the grain-boundary energy density. The sign convention for the curvature is that a convex surface has a negative curvature.

At the junction between a grain boundary and the surface, continuity of the chemical potential requires that

$$\sigma_{B0} = \kappa_0\gamma_S. \tag{4}$$

The effective stress of the film is the average of the normal stress along the grain boundary plus the in-plane component of the surface tension at the junction, namely,

$$\sigma_f = \frac{1}{h}\int_0^h \sigma_B(y)dy + \frac{\gamma_S}{h}\sin\psi. \tag{5}$$

Substituting Eq. (4) into Eq. (5), we obtain the residual film stress at the equilibrium state

$$\sigma_{\mathrm{EQ}} = \frac{\gamma_S}{h}(\kappa_0 h + \sin\psi). \tag{6}$$

The above stress is sometimes called zero-creep stress,[2] at which stress relaxation by diffusional creep stops. For a film with the dihedral angle close to 90°, the zero-creep stress is approximately γ_S/h, which can be significant for films of nanometer thickness[19] but negligible for thicker films with $h\sim 1$ μm.

B. Coupling of grain boundary and surface diffusion

At a nonequilibrium state, the gradient of the chemical potential drives atomic diffusion along the surface and the grain boundary. The atomic flux is given by the Nernst–Einstein equation, i.e.,

$$J_S = -\frac{\delta_S D_S}{\Omega kT}\frac{\partial\mu_S}{\partial s}, \tag{7}$$

$$J_B = -\frac{\delta_B D_B}{\Omega kT}\frac{\partial\mu_B}{\partial y}, \tag{8}$$

where δ_S is the thickness of the surface layer, D_S is the surface diffusivity, δ_B is the width of the grain boundary, D_B is

the grain-boundary diffusivity, k is Boltzmann's constant, and T is the absolute temperature.

On the free surface, local divergence of the atomic flux leads to change of the surface profile. Mass conservation requires that

$$v_n = -\Omega \frac{\partial J_S}{\partial s}, \tag{9}$$

where v_n is the normal velocity of the surface.

Let $\overline{y}(x,t)$ represent the surface profile. Combining Eqs. (1), (7), and (9) and approximately taking $v_n = \partial \overline{y}/\partial t$ and $\kappa = \partial^2 \overline{y}/\partial x^2$ by assuming that the slope of the surface is small everywhere, we obtain that

$$\frac{\partial \overline{y}}{\partial t} = -\frac{\delta_S D_S \gamma_S \Omega}{kT} \frac{\partial^4 \overline{y}}{\partial x^4}, \tag{10}$$

which is identical to the equation in the original analysis of grain-boundary grooving by Mullins.[20]

Similarly, the divergence of the atomic flux along a grain boundary causes a change in the normal stress. Thouless[15] assumed that the grain boundary remains planar, leading to a linear distribution of the flux that requires sliding at the film/substrate interface. Gao *et al.*[16] eliminated such sliding by considering the cracklike opening displacement and solving the grain-boundary stress using an edge dislocation model. Recent atomistic simulations by Buehler *et al.*[21] showed that atoms inserted into a grain boundary instantaneously crystallize and add to either one of the two grains joined by the grain boundary, rendering the structure of the grain boundary invariant. As a continuum description of this behavior, we assume that the mass insertion or removal due to the divergence of mass transport at the grain boundary induces an inelastic strain (or creep strain), ε_p, in the plane parallel to the film-substrate interface. By mass conservation, we have

$$\frac{\partial \varepsilon_P}{\partial t} = -\frac{\Omega}{l} \frac{\partial J_B}{\partial y}. \tag{11}$$

Due to the constraint of the substrate, the total in-plane strain of the film remains constant under the isothermal condition. Consequently, the change of the inelastic strain leads to a change in the elastic strain and thus the normal stress at the grain boundary. Neglecting other mechanisms for inelastic deformation and assuming linear elastic grains, we obtain that

$$\frac{\partial \sigma_B}{\partial t} = \frac{M\Omega}{l} \frac{\partial J_B}{\partial y}, \tag{12}$$

where M is the elastic modulus of the film.

Combining Eqs. (2), (8), and (12), we obtain that

$$\frac{\partial \sigma_B}{\partial t} = \frac{M\Omega \delta_B D_B}{lkT} \frac{\partial^2 \sigma_B}{\partial y^2}, \tag{13}$$

which is a standard diffusion equation in terms of the grain-boundary stress. Equation (13) is identical to the linear spring model proposed by Guduru *et al.*[22] for compressive stress evolution during thin-film growth. Similar models have been used by Chuang and Rice[23] and Sheldon *et al.*[24] In particular, Guduru *et al.*[22] compared the model with the dislocation model by Gao *et al.*[16] and found that the two models are in surprisingly good agreement despite the simplicity of the linear spring model.

Equations (10) and (13) describe the surface and grain-boundary diffusion, respectively, and they are coupled at the junction joining the free surface with a grain boundary, where the continuity of chemical potential and mass flux requires that

$$\left.\frac{\partial^2 \overline{y}}{\partial x^2}\right|_{x=0} = \frac{\sigma_B(h,t)}{\gamma_S}, \tag{14}$$

$$2J_S(x=0) = J_B(y=h). \tag{15}$$

Furthermore, the dihedral angle is always maintained by the local equilibrium, i.e.,

$$\left.\frac{\partial \overline{y}}{\partial x}\right|_{x=0} = \cot \psi. \tag{16}$$

In addition, we assume the following boundary conditions:

$$\left.\frac{\partial \sigma_B}{\partial y}\right|_{y=0} = 0, \tag{17}$$

$$\left.\frac{\partial \overline{y}}{\partial x}\right|_{x=l/2} = 0, \tag{18}$$

$$\left.\frac{\partial^3 \overline{y}}{\partial x^3}\right|_{x=l/2} = 0. \tag{19}$$

Equation (17) implies no atomic flux at the root of the grain boundary. Equations (18) and (19) represent a zero slope and a zero flux at the center of the grain surface as required by symmetry.

C. Numerical solution

A numerical method is developed to simultaneously solve Eqs. (10) and (13) with the conditions (14)–(19). Start with a stress distribution along the grain boundary, $\sigma_B(y,t)$, and a surface profile, $\overline{y}(x,t)$, at time t. The chemical potentials at the surface and the grain boundary are calculated using Eqs. (1) and (2). Next, the atomic flux is obtained from Eqs. (7) and (8). The surface profile and the stress distribution are then updated according to Eqs. (9) and (12), subjected to the boundary conditions in (14)–(19). The procedures repeat for many steps to simultaneously evolve the stress distribution at the grain boundary and the surface profile. We employ an explicit algorithm with a central-space-forward-time (CSFT) finite difference method and a sufficiently small time step to ensure the stability of the method. An unconditionally stable algorithm may be developed, but will not be pursued here. The initial condition for the grain-boundary stress and the surface profile depends on the thermal process history and is generally uncertain. For simplicity, we assume that the film initially has a uniform stress along the grain boundary and an equilibrium surface profile $\overline{y_0}(x)$ with the constant curvature κ_0.

Special attention is paid to ensure continuity of the chemical potential and the atomic flux at the junction be-

tween the grain boundary and the surface. Applying the finite difference approximation to Eqs. (14)–(16), and solving two coupled algebraic equations, we obtain that

$$\sigma_B^{(N)} = \frac{\sigma_B^{(N-1)} + 3\alpha_S\kappa_0\gamma_S}{1+3\alpha_S} - \frac{2\alpha_S\gamma_S}{(1+3\alpha_S)\Delta x^2}[u^{(2)} - u^{(3)}], \tag{20}$$

and

$$u^{(1)} = \frac{\Delta x^2}{2\gamma_S}\frac{\kappa_0\gamma_S - \sigma_B^{(N-1)}}{1+3\alpha_S} + \frac{(1+4\alpha_S)u^{(2)} - \alpha_S u^{(3)}}{1+3\alpha_S}, \tag{21}$$

where $\sigma_B^{(N)}$ is the grain-boundary stress at the junction, $\sigma_B^{(N-1)}$ is the stress at the node immediately below the junction, $u^{(1)}$, $u^{(2)}$, $u^{(3)}$ are the vertical displacements from the equilibrium surface profile, i.e., $u(x,t)=\overline{y}(x,t)-\overline{y_0}(x)$, at the first three nodes starting from the junction, Δx and Δy are finite difference spacings between adjacent nodes along the surface and the grain boundary, respectively, and $\alpha_S=(\delta_S D_S/\delta_B D_B)\times(\Delta y/\Delta x)$. The chemical potential at the junction can be obtained using either (20) and (21). The atomic flux at the junction is

$$J_X = -\frac{1}{kT}\left(\frac{\Delta y}{\delta_B D_B} + \frac{\Delta x}{3\delta_S D_S}\right)^{-1} \times\left\{\kappa_0\gamma_S - \sigma_B^{(N-1)} - \frac{2\gamma_S}{3\Delta x^2}[u^{(2)} - u^{(3)}]\right\}. \tag{22}$$

Figure 2 shows the numerical solution for the evolution of the surface profile and the grain-boundary stress with $\delta_S D_S/\delta_B D_B=1$. The time is normalized by a time constant

$$\tau_B = \frac{4kTh^2 l}{\pi^2 M\Omega\delta_B D_B}, \tag{23}$$

which is the characteristic time for the grain-boundary diffusion and will be discussed later. The parameters used in the calculation are $\sigma_0/M=0.001$, $h/l=1.0$, $Mh/\gamma_S=10^5$, and $\kappa_0=0$. Under tension, the surface profile develops grain-boundary grooving at the initial stage of relaxation. The depth of the grooving depends on the surface diffusivity and the initial tensile stress. Further relaxation refills the groove. Similarly, under compression, the surface profile develops hillocks at the junction. The grain-boundary stress relaxes in a manner of a typical diffusion process, which starts at the junction with the free surface and propagates into the film.

The effective stress of the film is calculated using Eq. (5) and plotted in Fig. 3 as a function of time for various ratios between the surface diffusivity and the grain-boundary diffusivity. It can be seen that the relaxation curve is insensitive to the surface diffusivity as long as $(\delta_S D_S/\delta_B D_B)>1$. In such cases, the surface diffusion may be approximately taken to be infinitely fast, for which a closed-form solution will be obtained below and is plotted in Fig. 3 as the dashed line. On the other hand, the relaxation curve becomes more sensitive to surface diffusivity when $(\delta_S D_S/\delta_B D_B)<1$.

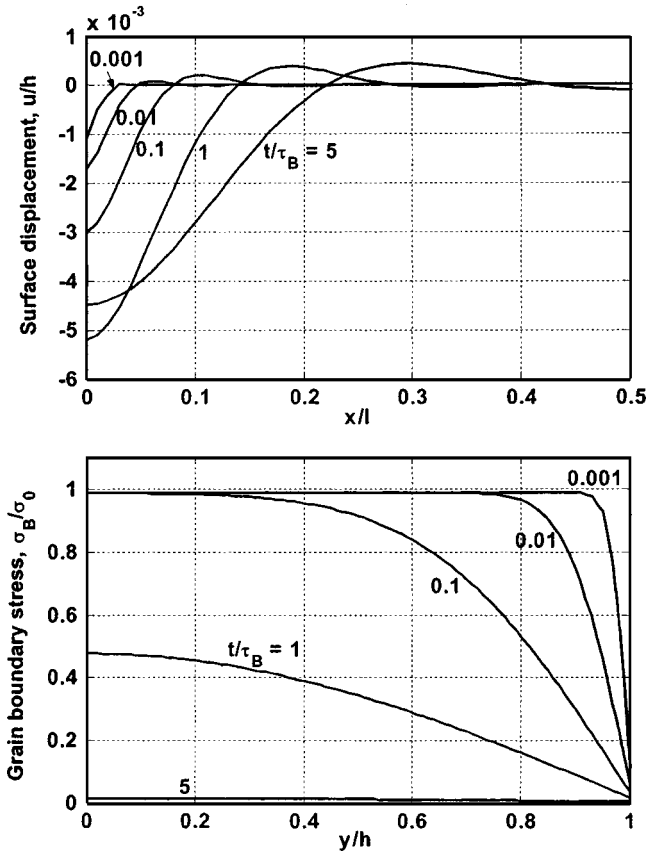

FIG. 2. Evolution of the surface profile and the normal stress at a grain boundary during isothermal relaxation of an unpassivated film with $\delta_S D_S/\delta_B D_B=1$.

D. Analytical solution for fast surface diffusion

Two limiting cases exist for the coupled diffusion problem. First, in the case of infinitely fast surface diffusion, the finite difference approximations in Eqs. (20)–(22) reduce to $\sigma_B^{(N)}=\kappa_0\gamma_S$, $u^{(1)}=u^{(2)}=u^{(3)}$, and $J_X=-(\delta_B D_B/kT)[\kappa_0\gamma_S-\sigma_B^{(N-1)}]/\Delta y$. Consequently, the surface profile maintains the equilibrium curvature and the flux rate is controlled by the

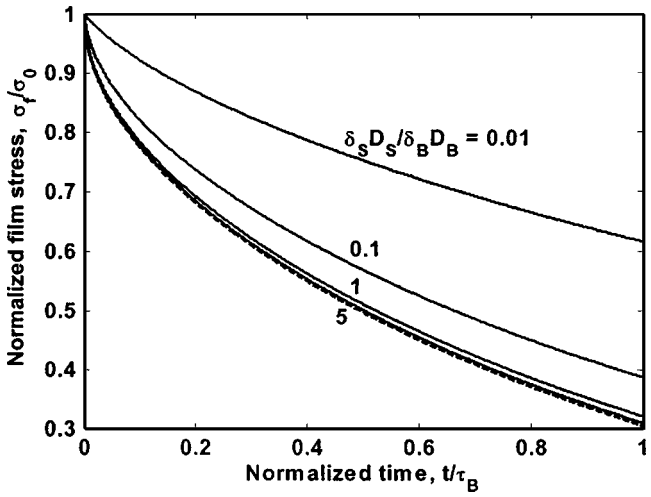

FIG. 3. Effect of surface diffusivity on stress relaxation of unpassivated films. The dashed line is for the limiting case with infinitely fast surface diffusion, predicted by Eq. (28).

grain-boundary diffusion. On the other hand, if grain-boundary diffusion is very fast compared to surface diffusion, we obtain $\sigma_B^{(N)}=\sigma_B^{(N-1)}=\gamma_S\kappa_S^{(1)}$, $u^{(1)}=u^{(2)}+\frac{1}{2}\Delta x^2[\kappa_0-\kappa_S^{(1)}]$, and $J_X=-(2\delta_S D_S\gamma_S/kT)[\kappa_S^{(2)}-\kappa_S^{(1)}]/\Delta x$, where $\kappa_S^{(1)}$ and $\kappa_S^{(2)}$ are the surface curvatures at the first two nodes near the junction. In this second limiting case, the stress along the grain boundary is always uniform and the kinetics is controlled by the surface diffusion. Analytical solutions can be obtained for both the limiting cases. Since surface diffusion is usually faster than grain-boundary diffusion, we present the analytical solution for the first limiting case below and give the solution for the second case in the Appendix for completeness.

Assuming infinitely fast surface diffusion, the continuity condition (14) reduces to

$$\sigma_B(y=h)=\kappa_0\gamma_S. \tag{24}$$

Solving Eq. (13) with the boundary conditions (17) and (24), we obtain that

$$\sigma_B(y,t)=\kappa_0\gamma_S+\sum_{n=0}^{\infty}A_n\cos(k_n y)\exp(-\bar{D}_B k_n^2 t), \tag{25}$$

where $\bar{D}_B=M\Omega\delta_B D_B/lkT$ and $k_n=[(2n+1)\pi]/2h$. The coefficients A_n can be determined from the initial distribution of the grain-boundary stress. Assuming that initially the grain-boundary stress is uniform and the effective film stress is σ_0, from Eq. (5), we obtain that

$$\sigma_B(t=0)=\sigma_0-\frac{\gamma_S}{h}\sin\psi. \tag{26}$$

Applying the initial condition (26) to Eq. (25) leads to

$$A_n=\frac{(-1)^n}{2n+1}\frac{4}{\pi}(\sigma_0-\sigma_{\mathrm{EQ}}), \tag{27}$$

where σ_{EQ} is the zero-creep stress given by Eq. (6).

The grain-boundary stress in Eq. (25) consists of a series expansion with each term decaying exponentially with time, similar to that obtained by Gao *et al.*,[16] but with different eigenfunctions and eigenvalues. In addition, the present solution includes the contribution from a zero-creep stress. A characteristic time scale emerges from the solution, given by Eq. (23), corresponding to the relaxation time for the first exponential term in Eq. (25). The evolution of the grain-boundary stress described by Eq. (25) is similar to the numerical solution shown in Fig. 2 with slight difference near the surface-grain-boundary junction.

Substitution of Eq. (25) into Eq. (5) leads to the effective film stress as a function of time

$$\sigma_f(t)=\sigma_{\mathrm{EQ}}+\frac{8(\sigma_0-\sigma_{\mathrm{EQ}})}{\pi^2}\sum_{n=0}^{\infty}\frac{\exp(-\bar{D}_B k_n^2 t)}{(2n+1)^2}. \tag{28}$$

Equation (28) describes the stress relaxation under an isothermal condition, which clearly exhibits a transient behavior: the rate of stress relaxation is fast initially but decreases as the higher-order terms decay exponentially at higher rates; after some time, only the first exponential term remains effective, corresponding to the steady-state creep. Eventually, the relaxation stops when the film stress reaches the zero-creep stress. Figure 4 plots the film stress as a function of time predicted by Eq. (28), in comparison with the steady-state solution by Thouless[15] and the approximate solution to the dislocation model for constrained grain-boundary diffusion by Gao *et al.*[16] While both the previous solutions predict exponential relaxation with very close stress rate, the present model predicts faster relaxation at the initial stage but slightly slower at the steady state.

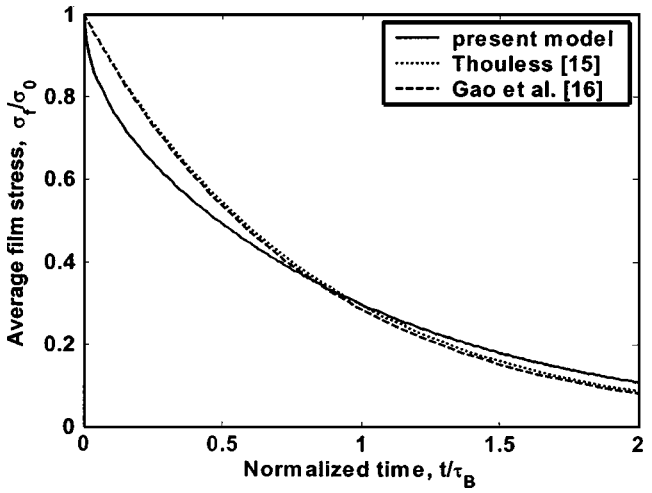

FIG. 4. Stress relaxation of an unpassivated film, predicted by Eq. (28), in comparison with the steady-state solutions from previous studies.

As indicated by the numerical solutions in Fig. 3, as far as the surface diffusion is faster than the grain-boundary diffusion, the analytical solution for the limiting case of infinitely fast surface diffusion can be used as a reasonable approximation. In Part I of this study we have compared the analytical solution to experimentally measured stress relaxation curves of unpassivated Cu films at different temperatures and initial stresses, and the agreement is reasonable. The grain-boundary diffusivity and its activation energy were extracted, which are in good agreement with other studies.

III. PASSIVATED FILMS: COUPLING OF GRAIN-BOUNDARY DIFFUSION AND INTERFACE DIFFUSION

For a passivated film [Fig. 1(b)], we assume that atoms diffuse along the grain boundary and the interface between the film and the passivation layer but neglect diffusion along the film-substrate interface. We further assume that the film-passivation interface remains flat all the time and the mass transport induces a locally nonzero normal stress at the interface, $\sigma_I(x)$, similar to the normal stress at the grain boundary. The mechanical equilibrium of the cap layer requires that the total normal stress at the interface be zero, i.e.,

$$\int_0^{l/2}\sigma_I(x)dx=0. \tag{29}$$

We define the chemical potential at the interface similar to that at the grain boundary, namely,

$$\mu_I=\mu_0-\sigma_I(x)\Omega. \tag{30}$$

The atomic flux along the interface is given by

$$J_I = -\frac{\delta_I D_I}{\Omega kT}\frac{\partial \mu_I}{\partial x}, \tag{31}$$

where δ_I is the thickness of the interface and D_I is the interface diffusivity.

The mass insertion or removal at the interface due to divergence of the atomic flux can be accommodated in two ways, by deformation of the grains and by a rigid-body motion of the passivation layer. Assuming elastic grains (similar to the linear spring model for the grain-boundary stress[22]) and a rigid passivation layer, the local normal stress associated with the elastic deformation is

$$\frac{\partial \sigma_I}{\partial t} = \frac{M}{h}\left[\Omega\frac{\partial J_I}{\partial x} + \Delta(t)\right], \tag{32}$$

where $\Delta(t)$ is the displacement of the passivation layer perpendicular to the interface, assumed to be uniform for a rigid layer passivation. Inserting Eq. (32) into Eq. (29) and noting that the flux at the center ($x=l/2$) is zero by symmetry, we obtain that

$$\Delta(t) = \frac{2\Omega}{l}J_I(0,t). \tag{33}$$

Combining Eqs. (29)–(32) leads to

$$\frac{\partial \sigma_I}{\partial t} = \frac{M\Omega\delta_I D_I}{hkT}\frac{\partial^2 \sigma_I}{\partial x^2} + \frac{M}{h}\Delta(t), \tag{34}$$

which is a familiar diffusion equation with a time-dependent source term.

We assume the following boundary conditions:

$$\left.\frac{\partial \sigma_I}{\partial x}\right|_{x=l/2} = 0, \tag{35}$$

$$\left.\frac{\partial \sigma_I}{\partial x}\right|_{x=0} = \frac{\delta_B D_B}{2\delta_I D_I}\left.\frac{\partial \sigma_B}{\partial y}\right|_{y=h}, \tag{36}$$

$$\sigma_I(0,t) = \sigma_B(h,t). \tag{37}$$

Equation (35) implies no flux at the center, and Eqs. (36) and (37) ensure continuity of the flux and the chemical potential at the junction between the interface and a grain boundary. As before, the grain-boundary diffusion is governed by Eq. (13) plus the boundary condition, Eq. (17), for no flux at the film-substrate interface. The coupled problem is then solved numerically, following a similar procedure as that in the previous section.

Figure 5 shows the effect of interface diffusivity on stress relaxation predicted by the present model. Compared to Fig. 3, the stress relaxation is much more sensitive to the interface diffusivity for passivated films than it is to the surface diffusivity for unpassivated films. This is more so if the diffusivities follow the general trend, $\delta_S D_S > \delta_B D_B > \delta_I D_I$. Figure 6 shows the evolution of the interface stress and the grain-boundary stress for the case $\delta_I D_I/\delta_B D_B = 1$. Note that, under a tensile initial stress ($\sigma_0 > 0$), a biaxial tensile stress develops at the junction between the grain boundary and the interface (i.e., $x=0$ and $y=h$), which starts with a high level and decays as the film relaxes. Experiments have observed

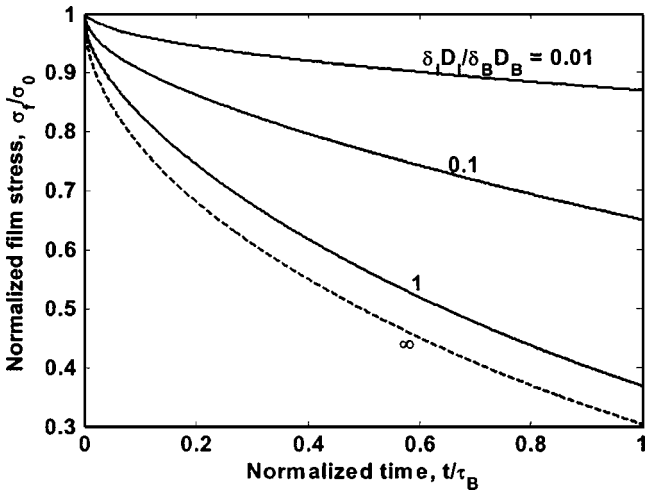

FIG. 5. Effect of interface diffusivity on stress relaxation of passivated films. The dashed line is for the limiting case with infinitely fast interface diffusion, predicted by Eq. (28).

voids in passivated Cu films,[25] but not in Al films covered with a native oxide. With interface diffusion in place, the present model predicts an equibiaxial stress at the junction in the plane of consideration as required by the continuity of chemical potential [i.e., Eq. (37)]. Such a stress state may be responsible for nucleation of voids at the grain-boundary junctions in Cu films. For Al films, however, the native oxide inhibits interface diffusion, thus no biaxial stress at the junction.

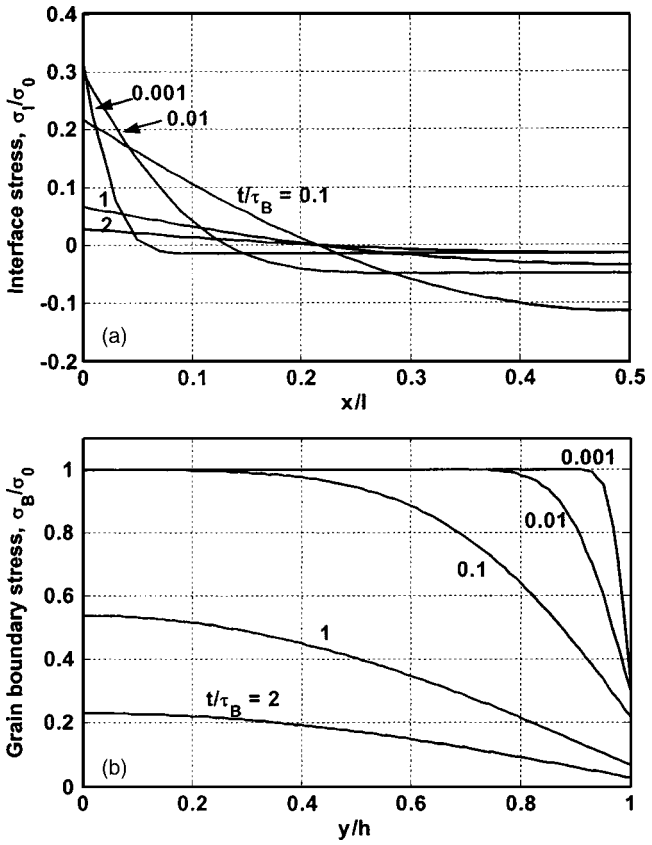

FIG. 6. Simulated evolution of (a) interface stress and (b) grain-boundary stress during isothermal relaxation of a passivated film with $\delta_I D_I/\delta_B D_B = 1$.

Similar to unpassivated films, there exist two limiting cases. First, if the interface diffusion is very fast, the normal stress along the interface remains zero, with all the mass insertion into or removal from the interface accommodated by the uniform rigid-body motion of the cap layer. Consequently, the solution is identical to that for unpassivated films with infinitely fast surface diffusion and zero equilibrium curvature ($\kappa_0=0$), as given by Eq. (28) and shown in Fig. 5 as the dashed line. On the other hand, if grain-boundary diffusion is very fast compared to the interface diffusion, the normal stress along the grain boundary remains constant, but depends on time. Similar to the solution presented in the Appendix for unpassivated films, we obtain a closed form solution for this limiting case,

$$\sigma_I(x,t) = \sigma_B(t) + \sum_{n=0}^{\infty} A_n \sin(k_n x)\exp(-\overline{D}_I k_n^2 t), \tag{38}$$

where

$$\overline{D}_I = \frac{M\Omega\delta_I D_I}{hkT}, \tag{39}$$

$$k_n l = (2n+1)\pi, \tag{40}$$

$$A_n = -\frac{4\sigma_0}{(2n+1)\pi}, \tag{41}$$

$$\sigma_B(t) = \sigma_0 \frac{8}{\pi^2}\sum_{n=0}^{\infty} \frac{\exp(-\overline{D}_I k_n^2 t)}{(2n+1)^2}. \tag{42}$$

The effective film stress, $\sigma_f(t)=\sigma_B(t)$, relaxes as described by Eq. (42), which is similar to Eq. (28), but with a different time scale

$$\tau_I = \frac{kThl^2}{\pi^2 M\Omega\delta_I D_I}. \tag{43}$$

Note that the time τ_I scales with hl^2 while the time τ_B in Eq. (23) scales with $h^2 l$. Similar time scales were obtained by Thouless[15] for surface-diffusion-controlled and grain-boundary-diffusion-controlled regimes, respectively. Gao *et al.*[16] predicted a characteristic time scaling with h^3 as a result of constrained grain-boundary diffusion. However, the eigenvalue associated with the time depends on the aspect ratio of the grain, therefore, not fundamentally different from the present time scales.

Figure 7 replots the numerical solutions for stress relaxation in Fig. 5 with the time now scaled by τ_I to compare with the closed-form solution for infinitely fast grain-boundary diffusion. It is noted that, while the rate of stress relaxation is sensitive to the interface diffusivity for $(\delta_B D_B/\delta_I D_I)<100$, it becomes insensitive when the ratio is larger.

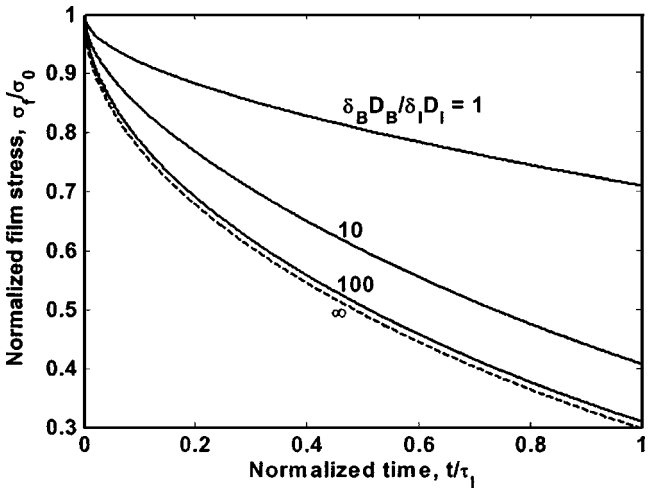

FIG. 7. Stress relaxation of passivated films. The dashed line is for the limiting case with infinitely fast grain-boundary diffusion, predicted by Eq. (42).

IV. DISCUSSIONS

As demonstrated in Part I, the present model captures essential features of experimental observations of isothermal stress relaxation in electroplated Cu films with and without a cap layer, including the transient behavior, the zero-creep stress, and the effect of interface diffusivity. However, we caution that the model should be used within a certain range of temperatures and stresses when the considered diffusion mechanism dominates the deformation process. For example, we found that the agreement between the model predictions and experiments is poor when the initial stress is high or when the temperature is high; in both cases, we expect other deformation mechanisms such as dislocation glide and power-law creep to intervene the process of interface-grain-boundary diffusion. It may be possible to determine the proper temperature-stress range for a particular mechanism through a systematic set of stress relaxation experiments at various temperatures and stress levels and construct a deformation mechanism map similar to those for bulk materials.[26]

Both the model and the experiments in this study clearly show the transient behavior of stress relaxation. Quantitatively, the transient stage predicted by the model is considerably shorter than that observed in experiments, which leads to an apparent discrepancy between the model prediction and the experiments at the initial stage of stress relaxation, especially for unpassivated films. This discrepancy may be attributed to the uncertainty of the initial condition. Our model analysis assumed that relaxation starts with a uniform normal stress along the grain boundaries and an equilibrium surface profile. However, in experiments, the starting point is selected based on the average stress during thermal cycling experiments, with no information on the stress distribution as well as the surface profile. In addition, it is also possible that other deformation mechanisms may contribute to the fast relaxation at the initial stage. For passivated films, the transient stage is shorter, resulting in a better agreement between experiments and the model.

Another point worthy of mentioning is the zero-creep stress. While the present model includes a zero-creep stress based on the equilibrium state for unpassivated films, the predicted value is much smaller than that extracted from experiments. The apparently larger zero-creep stress is not well understood. In comparison with experiments for unpassivated films, we used the analytical solution in Eq. (28) with

the experimentally extracted value for the zero-creep stress. For passivated films, it takes much longer to reach any zero-creep stress and the model assumes no zero-creep stress.

V. CONCLUDING REMARKS

We have modeled isothermal stress relaxation of unpassivated and passivated polycrystalline thin films by coupling grain-boundary diffusion with surface diffusion and interface diffusion, respectively. For unpassivated films, stress relaxation is insensitive to surface diffusivity if surface diffusion is faster than grain-boundary diffusion, in which case the closed-form solution for infinitely fast surface diffusion may be used to approximate the stress relaxation behavior. For passivated films, stress relaxation is much more sensitive to interface diffusivity, especially when interface diffusion is slower than grain-boundary diffusion. Consequently, isothermal stress relaxation tests may be used as a quantitative method to characterize kinetics of interface diffusion and to evaluate selected passivation layers for improving electromigration reliability of Cu interconnects.

Comparisons with experimental results in Part I have shown that the model is applicable for the electroplated Cu films within a certain range of the temperature and the stress level, when the diffusion mechanism dominates the deformation process in the Cu films. At a high stress level, however, other mechanisms such as dislocation glide and power-law creep may intervene the diffusion process. Systematic stress relaxation tests at various temperatures and stress levels may determine the proper range for the diffusion mechanism as well as other deformation mechanisms in thin films, similar to the deformation mechanism maps for bulk materials.[26] A better understanding is also needed for the transient behavior at the initial stage and the zero-creep stress.

ACKNOWLEDGMENTS

This work is supported by Advanced Technology Program of Texas Higher Education Coordinating Board and Intel Corporation. Discussions with J. Leu and J. He of Intel Corporation and H. Gao of Max-Planck Institute were very helpful.

APPENDIX: SOLUTION FOR UNPASSIVATED FILMS WITH INFINITELY FAST GRAIN-BOUNDARY DIFFUSION

In the limiting case of infinitely fast grain-boundary diffusion, the grain-boundary stress is always uniform, but depends on time, i.e., $\sigma_B(y,t)=\sigma_B(t)$. The surface diffusion is governed by Eq. (10) with the boundary conditions (16), (18), and (19) unchanged. In addition, the continuity of the chemical potential at the junction requires that

$$\left.\frac{\partial^2\overline{y}}{\partial x^2}\right|_{x=0}=\frac{\sigma_B(t)}{\gamma_S}. \tag{A1}$$

The atomic flux into or out of the grain boundary contributes to inelastic strain in the plane of the film. Due to the constraint by the substrate, the rate of the grain-boundary stress relates to the flux at the junction by

$$\frac{d\sigma_B}{dt}=\frac{2M\Omega}{hl}J_S(0,t). \tag{A2}$$

Equation (A2) may be understood as the integration of Eq. (12) with respect to y, noting that $J_B=0$ at $y=0$ and $J_B=2J_S(0,t)$ at $y=h$.

Conditions (A1) and (A2) combine to provide a mixed boundary condition, namely,

$$\left(\frac{\partial^3\overline{y}}{\partial x^2\partial t}-\frac{2M\Omega\delta_S D_S}{kThl}\frac{\partial^3\overline{y}}{\partial x^3}\right)_{x=0}=0. \tag{A3}$$

The solution to Eq. (10) takes the form

$$\overline{y}(x,t)=\overline{y_0}(x)+\sum_{n=1}^{\infty}A_n f_n(x)\exp(-\lambda_n t), \tag{A4}$$

where $\overline{y_0}(x)$ is the equilibrium profile of the surface, λ_n is the eigenvalue, and $f_n(x)$ the corresponding eigenfunction. Applying the boundary conditions, we obtain that

$$\overline{y_0}(x)=h-\tfrac{1}{2}\kappa_0 x(l-x), \tag{A5}$$

$$\lambda_n=k_n^4\frac{\delta_S D_S\gamma_S\Omega}{kT}, \tag{A6}$$

$$f_n(x)=\cos\left(k_n x-\frac{k_n l}{2}\right)+2\exp\left(-\frac{k_n l}{2}\right)\sin\left(\frac{k_n l}{2}\right)\times\cosh\left(k_n x-\frac{k_n l}{2}\right), \tag{A7}$$

where $k_n l$ is the nth solution to the following transcendental equation:

$$x^3\left[1-\cot\left(\frac{x}{2}\right)\right]=\frac{4Ml^2}{\gamma_S h}. \tag{A8}$$

Note that the eigenfunction (A7) satisfies the boundary condition (16) approximately under the assumption $k_n l\gg 1$. It can be shown that, for typical values of h/l (~ 1) and Mh/γ_S ($\gg 1$), the smallest solution to Eq. (A8) is approximately $k_1 l\approx 2\pi$, making $k_n l\gg 1$ a reasonable assumption.

Assume that the surface curvature initially takes the equilibrium value κ_0 everywhere except at the grain-boundary junction, where the continuity of chemical potential requires condition (A1). Consequently, we have

$$\left.\frac{\partial^2\overline{y}}{\partial x^2}\right|_{t=0}=\frac{\sigma_{B0}}{\gamma_S}-\left(\frac{\sigma_{B0}}{\gamma_S}-\kappa_0\right)H(x), \tag{A9}$$

where σ_{B0} is the initial grain-boundary stress, and $H(x)$ is the Heaviside function. Taking the derivative of Eq. (A9), we obtain that

$$\left.\frac{\partial^3\overline{y}}{\partial x^3}\right|_{t=0}=-\left(\frac{\sigma_{B0}}{\gamma_S}-\kappa_0\right)\delta(x), \tag{A10}$$

where $\delta(x)$ is the Dirac delta function. Equation (A10) implies an infinite flux rate at the junction, which is the result of the discontinuity of the initial chemical potential assumed in Eq. (A9).

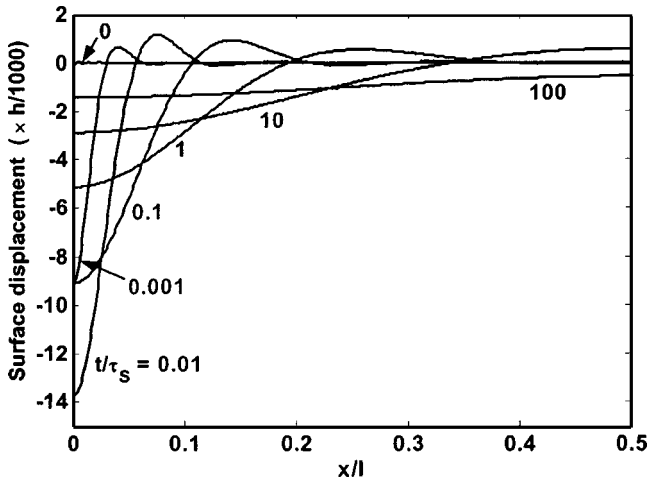

FIG. 8. Evolution of surface profile of an unpassivated film with infinitely fast grain-boundary diffusion.

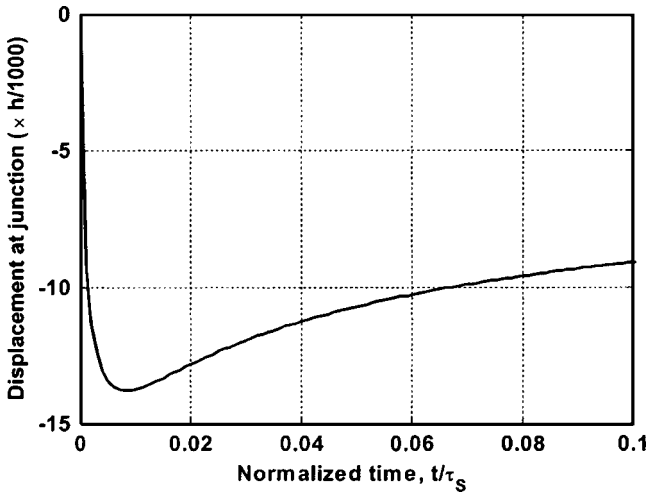

FIG. 9. Displacement at the grain-boundary junction (grooving) as a function of time for an unpassivated film with infinitely fast grain-boundary diffusion.

It can be shown that the third derivatives of the eigenfunctions (A7) are orthogonal, i.e.,

$$\int_0^{l/2} f_n'''(x) f_m'''(x) dx = 0 \quad \text{for } m \neq n. \tag{A11}$$

Thus, the coefficients A_n in Eq. (A4) can be determined from the initial condition (A10), namely,

$$A_n = -\left(\frac{\sigma_{B0}}{\gamma_S} - \kappa_0\right) \frac{\int_0^{l/2} \delta(x) f_n'''(x) dx}{\int_0^{l/2} [f_n'''(x)]^2 dx}. \tag{A12}$$

Inserting Eq. (A7) into Eq. (A12), we obtain that

$$A_n = h \frac{\sigma_{B0} - \kappa_0 \gamma_S}{M} a\left(\frac{k_n l}{2}\right), \tag{A13}$$

where a is a dimensionless number given by

$$a(x) = \frac{4x(\sin x - \cos x)}{2x + 3(1 - \sin 2x - \cos 2x)}. \tag{A14}$$

Substitution of Eq. (A4) into Eq. (A1) leads to the grain-boundary stress as a function of time

$$\sigma_B(t) = \kappa_0 \gamma_S + (\sigma_{B0} - \kappa_0 \gamma_S) \sum_{n=1}^{\infty} \frac{4}{k_n l} \sin\left(\frac{k_n l}{2}\right) a\left(\frac{k_n l}{2}\right) \times \exp(-\lambda_n t). \tag{A15}$$

The relaxation of grain-boundary stress predicted by Eq. (A15) takes a similar form as that in Eq. (28), but has a different time scale depending on the surface diffusivity, i.e., $\tau_S = kTh l^2 / M\Omega\delta_S D_S$. Figure 8 shows the evolution of the surface profile for $\sigma_{B0}/M = 0.001$. Other parameters used in the calculation are $h/l = 1.0$, $Mh/\gamma_S = 10^5$, and $\kappa_0 = 0$. Compared to Fig. 2, the fast grain-boundary diffusion leads to enhanced grooving under tension. After a sufficiently long time, the stress is completely relaxed and the mass transport between the surface and the grain boundary results in a uniform surface displacement ($= -h\sigma_{B0}/M$). Figure 9 shows the displacement at the grain-boundary junction as a function of time. The maximum depth of grooving scales with the initial stress.

[1] O. Kraft, L. B. Freund, R. Phillips, and E. Arzt, MRS Bull. **27**, 30 (2002).
[2] D. Josell, T. P. Weihs, and H. Gao, MRS Bull. **27**, 39 (2002).
[3] Z. Suo, in *Comprehensive Structural Integrity*, edited by I. Milne, R. O. Ritchie, and B. Karihaloo, Vol. 8: Interfacial and Nanoscale Failure (Elsevier, Amsterdam, 2003), pp. 265–324.
[4] J. W. Hutchinson and Z. Suo, Adv. Appl. Mech. **29**, 63 (1992).
[5] R. M. Keller, S. P. Baker, and E. Arzt, Acta Mater. **47**, 415 (1999).
[6] M. D. Thouless, J. Gupta, and J. M. E. Harper, J. Mater. Res. **8**, 1845 (1993).
[7] R. P. Vinci, E. M. Zielinski, and J. C. Bravman, Thin Solid Films **262**, 142 (1995).
[8] C. K. Hu, R. Rosenberg, and K. Y. Lee, Appl. Phys. Lett. **74**, 2945 (1999).
[9] P. Besser, A. Marathe, L. Zhao, M. Herrick, C. Capasso, and H. Kawasaki, Tech. Dig. - Int. Electron Devices Meet.**2000**, 119.
[10] M. J. Kobrinsky, C. V. Thompson, and M. E. Gross, J. Appl. Phys. **89**, 91 (2001).
[11] D. W. Gan, S. Yoon, P. S. Ho, P. Cresta, N. Singh, A. F. Bower, J. Leu, and S. Shankar, Proc. Int. Interconnect Technology Conference (San Francisco, 2003).
[12] J. R. Rice and T. J. Chuang, J. Am. Ceram. Soc. **64**, 46 (1981).
[13] F. Y. Genin, W. W. Mullins, and P. Wynblatt, Acta Metall. Mater. **41**, 3541 (1993).
[14] Y. A. Antipov and H. Gao, Proc. R. Soc. London, Ser. A **458**, 1673 (2002).
[15] M. D. Thouless, Acta Metall. Mater. **41**, 1057 (1993).
[16] H. Gao, L. Zhang, W. D. Nix, C. V. Thompson, and E. Artz, Acta Mater. **47**, 2865 (1999).
[17] L. Zhang and H. Gao, Z. Metallkd. **93**, 417 (2002).
[18] A. F. Bower, N. Singh, D. Gan, S. Yoon, P. S. Ho, J. Leu, and S. Shankar, J. Appl. Phys. **97**, 013539 (2005).
[19] K. E. Harris and A. H. King, Acta Mater. **46**, 6195 (1998).
[20] W. W. Mullins, J. Appl. Phys. **28**, 333 (1957).
[21] M. J. Buehler, A. Hartmaier, and H. Gao, J. Mech. Phys. Solids **51**, 2105 (2003).
[22] P. R. Guduru, E. Chasen, and L. B. Freund, J. Mech. Phys. Solids **51**, 2127 (2003).
[23] T. J. Chuang and J. R. Rice, Acta Metall. **21**, 1625 (1973).
[24] B. W. Sheldon, A. Ditkowski, R. Beresford, E. Chason, and J. Rankin, J. Appl. Phys. **94**, 948 (2003).
[25] T. M. Shaw, L. Gignac, X. H. Liu, and R. R. Rosenberg, in *Stress-Induced Phenomena in Metallization, Sixth International Workshop*, edited by S. P. Baker, M. A. Korhonen, E. Artz, and P. S. Ho, AIP Conf. Proc. No. 612 (AIP, Melville, NY, 2002, pp. 177–183.
[26] H. J. Frost and M. F. Ashby, *Deformation-Mechanisms Maps* (Pergamon, Oxford, 1982).